Analyst

ROYAL SOCIETY OF CHEMISTRY

PAPER

Cite this: *Analyst*, 2021, **146**, 7160

Multi-layered polymer cantilever integrated with full-bridge strain sensor to enhance force sensitivity in cardiac contractility measurement†

Dong-Su Kim,[a] Yun-Jin Jeong,[a] Jongsung Park,[b] Arunkumar Shanmugasundaram[a] and Dong-Weon Lee *[a,c,d]

In this study, we developed a multi-layered functional cantilever for real-time force measurement of cardiomyocytes in cell culture media. The functional cantilever with a full-bridge circuit configuration was composed of one polydimethylsiloxane (PDMS) and two polyimide (PI) layers, forming two resistive sensors on each upper side of the two PI layers. The PI layers were chemically bonded using an oxygen plasma treatment, with a thin composite layer consisting of Cr/SiO_2/PDMS. These greatly improved the force sensitivity and the long-term reliability of the integrated strain sensor operating in liquids. The nano-grooved PDMS top layer bonded on the upper PI layer was employed to further improve the growth of cardiomyocytes on the functional cantilever. The difference in resistance changes and response characteristics was confirmed by evaluating the characteristics of the multi-layered polymer cantilevers with half-bridge and full-bridge circuit configurations. We also employed the cantilever devices to measure the contraction force of cardiomyocytes for 16 days and side effects in real time in human-induced pluripotent stem cells treated with the cardiovascular drug verapamil. The sensor-integrated cantilever devices are expected to be utilized as a novel biomedical sensor for evaluating the mechanobiology of cardiomyocytes, as well as in drug screening tests.

Received 6th July 2021,
Accepted 30th September 2021

DOI: 10.1039/d1an01208h

rsc.li/analyst

1. Introduction

To date, numerous cantilever-based biosensors have been proposed to measure the contractility of the cultured cardiomyocytes.[1] For instance, several forms of SU-8 cantilever such as surface patterned, spiral shaped, micro-patterned with metal electrodes, interdigitated electrode arrays, and PI-based microcantilevers have been proposed to measure the drug-induced changes in the contractility of the cardiomyocytes.[2–6] Feinberg *et al.* proposed PDMS muscular thin film (MTS) and analyzed the curvature of a thin film due to cyclic contraction of cardiomyocytes through an image-processing technique.[7] Although these biosensing platforms exhibit excellent sensing characteristics, most of the proposed cantilevers are rely on optical methods to measure the contraction force of the cardiomyocytes. The optical method is data intensive and not suitable for parallelized measurements. Besides, high-throughput real-time measurement is almost impossible.

To overcome the limitations of the optical-based measurement system, strain sensor integrated microcantilever platforms have been proposed for biomedical applications.[6,8–12] Integration of the strain sensors into the cantilever makes measurement more convenient and easier to use.[13] To the best of our knowledge, there are only six reports on strain sensor integrated microcantilever platforms for preliminary drug screening applications. For example, Kim *et al.* developed a piezoresistive strain sensor-integrated PDMS microcantilever platform.[8] Lind *et al.* proposed a Ti/Au metal strain sensor patterned PDMS MTS.[10] However, the drawbacks of these platforms are the formation of microcracks in the metal pattern owing to the low Young's modulus and high thermal coefficient of PDMS, which limits the long-term durability of the sensing platform. Kim *et al.* circumvented this limitation by preparing a wrinkle-free Cr/Au strain sensor on a PI microcantilever and successfully used it to detect long-term drug-induced changes in cardiac contractility.[6] The disadvantage of the Cr/Au integrated PI/PDMS microcantilever is its low sensitivity. An extremely durable and sensitive nano-crack sensor

[a]*School of Mechanical Engineering Chonnam National University, Gwangju, 61186, Republic of Korea. E-mail: mems@jnu.ac.kr*
[b]*Department of Precision Mechanical Engineering Kyungpook National University, Sangju, Gyeongsangbuk-do, 37224, Republic of Korea*
[c]*Center for Next-Generation Sensor Research and Development Chonnam National University, Gwangju 61186, Republic of Korea*
[d]*Advanced Medical Device Research Center for Cardiovascular Disease, Chonnam National University, Gwangju 61186, Republic of Korea*
†Electronic supplementary information (ESI) available. See DOI: 10.1039/d1an01208h

embedded in a silicone rubber cantilever has been proposed for the detection of small changes in cardiomyocyte contractility.[9] The primary disadvantage of this device is its non-linear behavior. Besides, this device cannot be used in strain ranges of more than 2% because the cracks completely open and the crack sensor's resistance cannot be measured. Lind *et al.* proposed a new type of cardiac microphysiological device prepared using a carbon black composite and 3D printing technology.[11] Despite the excellent sensor stability and durability, its sensitivity was significantly restricted by the limitation of the fabricable thickness of the cantilever body and sensor. Matsudaira *et al.* achieved a high sensing resolution (less than 0.1 nN) using a doped silicon (Si) sensor.[12] The high Young's modulus of Si (~150 GPa) reduces the displacement of the cantilever and it is not suitable for measuring very weak forces such as cardiac contractility. Therefore, developing a highly sensitive and reliable strain sensor on a polymer cantilever is essential for precisely monitoring the contractile force of cardiomyocytes.

Herein, we developed a multi-layered polymer cantilever integrated with a full-bridge configuration strain sensor for measuring the contractile force of cardiomyocytes. The multi-layered polymer cantilever was composed of a bottom and a top PI layer, a sandwiched PDMS layer and an encapsulation layer. Each set of strain sensors was patterned on the bottom and top PI layers using a lift-off process. The pair of strain sensors formed on each PI layer was configured as a full-bridge configuration that confers higher sensitivity compared with single and half-bridge configurations. Each PI layer was chemically bonded through a PDMS sandwich layer to enable a reliable operation in liquid conditions such as culture media. Following basic experimentation with the prepared cantilevers, we measured the contractile force as a function of the culture day and investigated biological behaviour such as the force–frequency relationship (FFR) to demonstrate the advantages of the proposed multi-layered polymer cantilever device. This cantilever device integrated with the full-bridge sensor is expected to be used in drug toxicity testing through a systematic analysis of cardiac contractility.

2. Materials and methods

2.1 Device concept of the multi-layered polymer cantilever

The proposed multi-layered polymer cantilever consists of three active layers, namely the bottom PI, top PI, and an encapsulation nanogrooved PDMS layer, and one passive sandwiched PDMS layer. In the conventional photolithography process, integration of strain sensors on both sides of the same substrate is more complicated. Hence, two Cr/Au strain sensors are integrated on the bottom PI and another two are integrated on the top PI layer. However, the chemical bonding of these two Cr/Au strain sensor integrated PI layers is highly impossible. Therefore, the Cr/Au strain sensor integrated two PI layers were chemically bonded together using the Cr/SiO_2 adhesion layer and sandwiched PDMS layer. Generally, adhesion of SiO_2 on the Au (Cr/Au-strain sensor) is significantly low. Therefore a 2 nm Cr buffer layer was deposited on the Cr/Au deposited PI. Then, a 3 nm SiO_2 layer was deposited on the 2 nm Cr layer. Next, 5 μm sandwiched PDMS was chemically bonded through the SiO_2 using oxygen plasma treatment. The oxygen plasma treatment enables the active oxygen functional groups on the surface of the PDMS and SiO_2, which is beneficial for chemical bonding. The same concept was utilized to chemically bond between the sandwiched PDMS layer and top PI layer.

Besides, the PI layer has certain limitations for use in cell experiments owing to its high Young's modulus. This is because biomaterials, similar to the elastic modulus of soft tissues, are more effective in studying the mechanophysiology of cells. Therefore, the softer material such as the nanogrooved PDMS encapsulation layer was bonded on the top PI layer using the same technique (Cr/SiO_2 adhesion layer) as described in the earlier section. The PDMS encapsulation layer not only acts as a cell culturing substrate but also protects the Cr/Au strain sensor from culture media exposure. By realizing this device concept, we ended up with the multi-layered polymer cantilever structure. The thickness of each polymer layer was optimized through finite element analysis (Fig. S1 and S2†). Table S1 in the ESI† shows the various parameters that have been used to optimize the cantilever layer thickness.

2.2. Working principle of the full-bridge strain sensor integrated multi-layered polymer cantilever

Fig. 1 presents the working principle of the multi-layered polymer cantilever integrated with the full-bridge configuration. Cardiomyocytes were cultured on the nanopatterned PDMS surface of the cantilever, and they produced repeated surface stresses on the cantilever surface during growth (Fig. 1a). The strain sensor was placed on both the top and bottom PI layers, forming the full bridge configuration (Fig. 1b and c). The strain sensor was configured such that it satisfied the initial conditions of the general Wheatstone bridge ($R_1 \cdot R_4 = R_2 \cdot R_3$). By supplying an input voltage through nodes 1 and 3 of the full-bridge configuration, (V_{in} = 1.2 V), a potential difference (V_{out}) was generated through nodes 2 and 4. R_1 and R_4 formed on the top PI surface were exposed to compressive stress during the repeated contraction of cardiomyocytes, while R_2 and R_3 formed on the bottom PI were subjected to the tensile properties of the thin film (Fig. 1d). The output voltage generated through the Wheatstone bridge configuration on the polymer cantilever increases during the systolic stage and decreases during the diastolic stage of cultured cardiomyocytes. The contraction force of the cardiomyocytes can be precisely quantified by measuring the change in output voltage of the Wheatstone bridge configuration (Fig. 1e).

2.3. Preparation of the Cr/Au strain sensor-integrated PI films

Fig. 2 depicts the process flow for the preparation of the multi-layered polymer cantilever. The first step of cantilever preparation was preparation of the PI film (thicknesses = 25 μm for the top plate and 12.5 μm for the bottom plate). For ease of

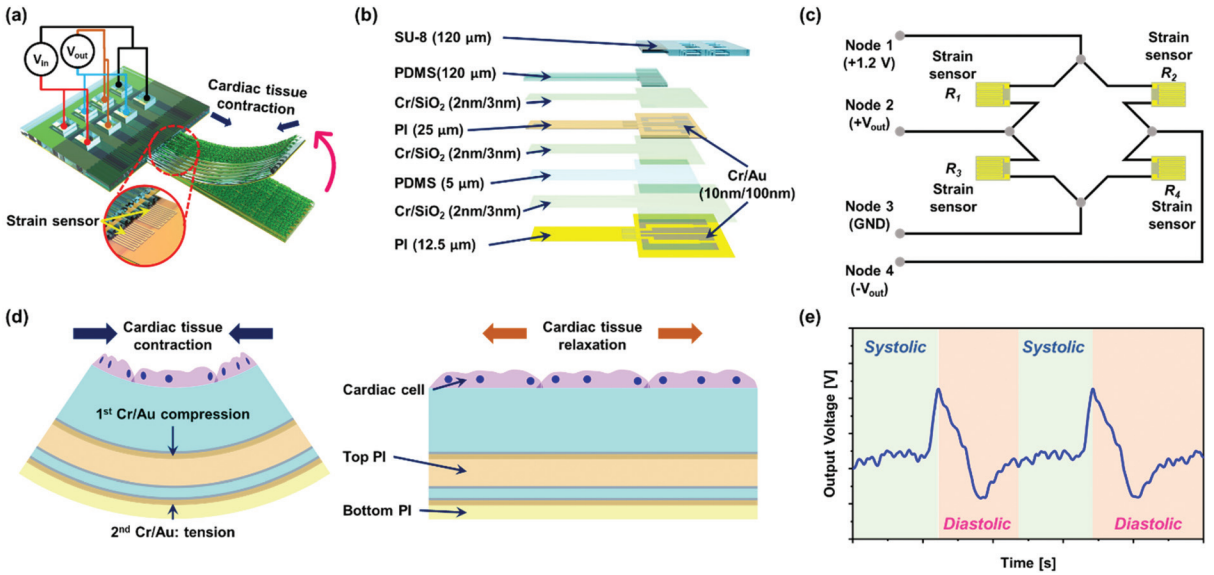

Fig. 1 Schematic illustration of the multi-layered polymer cantilever integrated with a full-bridge strain sensor. (a–c) Operation principles, cross-sectional diagram, and strain sensor configuration. (d) Detection principle for measuring the contraction and relaxation of cultured cardiomyocytes, and (e) change in output voltage resulting from the contraction and relaxation of cultured cardiomyocytes.

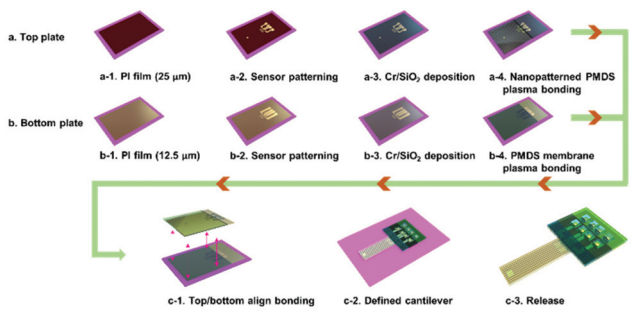

Fig. 2 Preparation process flow for the multi-layered polymer cantilever integrated with the full-bridge configuration.

handling, the PI film was attached to a Si wafer coated with a thin layer of PDMS as a soft adhesive. Subsequently, 10 nm and 100 nm thick chromium (Cr) and gold (Au) layers were deposited on each PI film at a deposition rate of 1 Å s^{-1} using an E-beam evaporator (base pressure: $\leq 5 \times 10^{-6}$). The sensor was subsequently patterned onto both PI films using the following preparation process. A photoresist (AZ-GXR 601 – 46 CP, positive tone) was spin-coated on the Cr/Au-deposited PI film at 4000 rpm for 40 s. Subsequently, soft baking was performed for 90 s using a preheated hot plate (90 °C). Next, the PI film was exposed to UV (12 mJ cm^{-2}) for 8 s using a double-side mask aligner (MDA-400M, MIDAS SYSTEM). A post-exposure bake (PEB) was performed for 90 s using the hot plate preheated to 110 °C. The photoresist was then developed for 50 s using an AZ 300 MIF developer, and the sensor patterns on the PI films were rinsed with deionized (DI) water for removing the residual developer and dried with nitrogen gas. Next, the Wheatstone bridge configuration on the PI films was defined through a wet chemical etching method using Cr and Au etchants. Finally, the photoresistor patterns were removed using acetone solution.

2.4. Preparation of the nanogroove-patterned PDMS encapsulation layer

In a typical preparation process of the nanogrooved PDMS encapsulation layer, firstly, we placed 5 mL of polyurethane acrylate (PUA), a UV-curable resin, on the 6-inch Si master mold with nanogrooves; this PUA was spin-coated at 1000 rpm for 40 s. The mold was then covered with a flexible film of polyethylene terephthalate substrate (PET, 125 μm thick), and the PUA solution diffused into the nanogroove was weakly cured by UV irradiation (~12 mJ cm^{-2}). After the PET substrate was peeled in the longitudinal direction of the nanogrooves, the PUA layer was exposed to UV light again for 10 h with an exposure energy of ~20 mJ cm^{-2} to complete the preparation of the nanogroove replication. The PDMS mixture was prepared by mixing the base polymer and a curing agent in a 10 : 1 ratio. The mixture was stored in a vacuum desiccator for 30 min for removing air bubbles. For ease of handling, the nanogroove-patterned PET film was attached to a Si wafer with a thin layer of PDMS as a soft adhesive. The PDMS mixture was spin-coated on the mold at 800 rpm for 40 s. Next, the PET film with the thin PDMS layer was cured for 1 h using a preheated hot plate (100 °C). After the curing process, the nanogroove-patterned PDMS film was peeled off from the PUA surface.

2.5. Preparation of the multi-layered polymer cantilever

In a typical preparation process, firstly, a 2 nm (deposition rate: 2.83 nm min^{-1}) thick Cr buffer layer was deposited on the bottom PI film with the strain sensor. Then, an SiO_2 layer was

deposited on the thin Cr layer using plasma-enhanced chemical vapor deposition (PECVD), as shown in Fig. S3a.† The thickness of the SiO_2 layer employed for plasma bonding to the PDMS was approximately 3 nm (deposition rate: 1.6 nm s^{-1}). The intermediate Cr layer was utilized for enhancing the adhesion of the SiO_2 and PDMS layer. The bottom PI film with Cr/SiO_2 layers was chemically bonded to the PDMS film (5 μm thick) using oxygen plasma treatment (CUTE-1MPR, Femto Science Inc.) at 90 W for 1 min under a 20 sccm oxygen atmosphere (Fig. S3b†). Next, a 2 nm (deposition rate: 2.83 nm min^{-1}) thick Cr layer was deposited on both sides of the top PI layer with another two strain sensors, and PECVD was used for depositing SiO_2 at a thickness of 3 nm (deposition rate: 1.6 nm s^{-1}) on the Cr layers, as shown in Fig. S3c.† The top PI film with the Cr/SiO_2 layers was bonded to the PDMS film on the bottom PI film using the abovementioned oxygen plasma treatment (Fig. S3c and d†). Finally, the nanogroove-patterned PDMS layer was chemically bonded to the top PI film (Fig. S3e and f†). The nanogrooves formed on the PDMS help the alignment and maturation of cardiomyocytes as they grow. SU-8 2050 was employed for forming the cantilever body, and the cantilever shape was defined using a roll-to-plate equipment (TSUKATANI, BFX) and a pinnacle die.

2.6 Neonatal rat ventricular myocyte (NRVM) isolation and cell culture

All animal experiments were performed following protocols approved by the Animal Ethics Committee at Chonnam National University in accordance with the Principles of Laboratory Animal Care and specific national laws (license number: CNU IACIC-YB-R-2015-1). Neonatal ventricular myocytes were isolated from the heart of Sprague-Dawley rats within days 1–3. The separated ventricles were washed using 1X ADS buffer solution (NaCl 120 mM, HEPES 20 mM, NaH_2PO_4 8 mM, D-glucose 6 mM, KCl 5 mM, $MgSO_4$ 0.8 mM, and DI water 1 L, pH 7.35). Single cardiomyocytes were isolated by treatment with an enzyme solution (collagenase 0.5 mg mL^{-1}, pancreatin 0.6 mg mL^{-1}, and 1× ADS buffer solution, 50 mL) and pre-plating. For effective coating with fibronectin (Corning®), the multi-layered polymer cantilever devices with the full-bridge strain sensor were exposed to an oxygen plasma system (FEMTO SCIENCE, 80 W, 30 s) for surface treatment. The isolated cardiomyocytes were subsequently seeded on the nanogrooved PDMS surface at a density of 1000 cells mm^{-2}. Finally, the cardiomyocytes seeded on the cantilever were cultivated at 37 °C in a 5% CO_2 incubator, and the culture medium was replaced every 72 h.

3. Results and discussion

3.1. Preliminary characteristics of the multi-layered polymer cantilever

Fig. 3a and b presents optical images of the prepared multi-layered polymer cantilever and the cross-sectional view of the cantilever composed of multiple polymer layers, respectively.

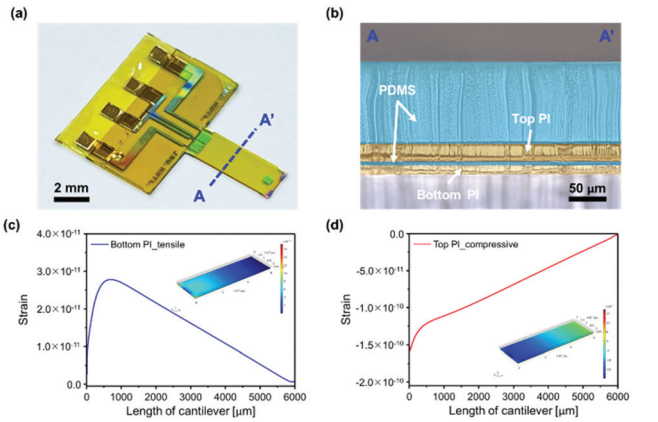

Fig. 3 (a) Optical images of the prepared polymer cantilever. (b) Optical image shows the cross-sectional view of the multi-layered polymer cantilever. (c and d) Finite element analysis of the strain along the cantilever length.

The dimensions of the cantilever are 6 mm × 2 mm × 0.14 mm, and the strain sensor is located 800 μm from its fixed end. Fig. 3c and d depicts the strain characteristics of the bottom and top PI films analyzed using a finite element method (COMSOL Multiphysics). A concentrated force was applied to the free end of the cantilever, generating 100 μm of displacement. The maximum strain value of the top PI film was approximately 3 times greater than that of the bottom PI film.

The strain of the substrate is proportional to the extent of change in the resistance of the integrated sensor. The change in resistance of the strain sensor at the bottom PI (R_2, R_3) and top PI (R_1, R_4) can be related to the output voltage of the Wheatstone bridge configuration according to eqn. (1). Therefore, the strain and the output voltage can be confirmed to be proportional to each other, and a larger strain difference between the bottom PI and top PI is theoretically confirmed to reflect a higher sensitivity.

$$V_{out} = \left(\frac{R_3}{R_1 + R_3} - \frac{R_4}{R_2 + R_4}\right) V_{in} \quad (1)$$

Furthermore, we experimentally confirmed that the sensitivity of the full-bridge sensor is increased because the upper sensor is subjected to compressive stress, while the lower part is subjected to tensile stress.

The resistance change (ΔR) and output voltage (V_{out}) of the full-bridge configuration were analyzed as a function of the displacement applied to the free end of the polymer cantilever. The ΔR of the strain sensor was measured using a LabVIEW-based data acquisition system (PXI-4071, National Instruments Inc., Austin, TX, USA). A programmable motorized stage was used to produce a desirable displacement at the free end of the cantilever to reproduce a contraction and relaxation behavior similar to that of cardiomyocytes. Fig. 4a presents the movement of the motorized stage, which moved 100 μm from the initial position to the +Z axis at 1 s intervals. The character-

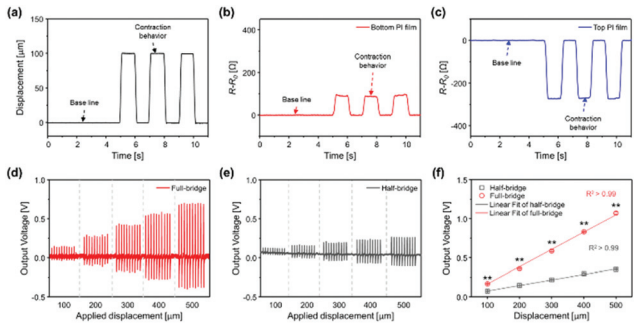

Fig. 4 Preliminary characterization of integrated strain sensors with half- and full-bridge configurations on the polymer cantilever. (a) Cantilever displacement generated by a motorized stage. (b) Changes in resistance as a function of cantilever displacement for the strain sensor formed on the bottom PI film and (c) top PI film. (d and e) Change in output voltage under conditions of pulsed displacement ranging from 100–500 μm. (f) Sensor linearity in output voltage with respect to the applied displacement.

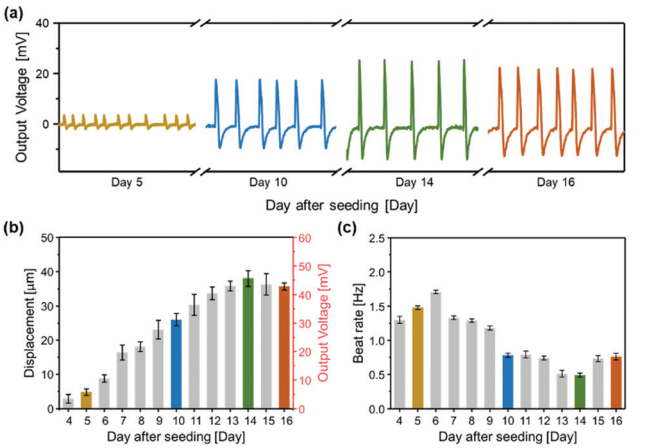

Fig. 5 Representative traces of cardiomyocytes cultured on the proposed cantilever. (a) Real-time cantilever array output voltage obtained from a single well on day 14. (b) Bar plot depicting sensor output voltage at different cell culture periods from day 4 to day 16. (c) The beat rate generated by the cultured cardiomyocytes from day 4 to day 16.

istics' evaluation was performed using three different cantilevers to prove the repeatability and reliability of the prepared strain sensor. When a displacement of 100 μm was applied, the ΔR of the strain sensor integrated on the bottom and top PI films was determined to be ~91 ± 2.15 and 272 ± 1.69 mΩ, respectively (Fig. 4b and c). As a structural characteristic of the proposed multi-layered polymer cantilever, the strain sensor integrated on the bottom PI film showed an increase in resistance (exposed to tensile stress) against the applied displacement, and the strain sensor integrated on the top PI film exhibited a resistance decrease (exposed to compressive stress). The resistance change (ΔR) of the strain sensor was proportional to the strain values on the surface of both PI films. When the motorized stage was moved back to its initial position, the resistance reverted to the baseline value without any hysteresis. The maximum strain value obtained by the integrated strain sensor on the top PI layer was approximately 3 times greater than that for the bottom PI. This result was not significantly different from the theoretical result obtained in the FEM analysis. Fig. 4d shows the output voltage of the full-bridge configuration for different displacements in the range of 100–500 μm. The measured output voltages at 100 and 500 μm were ~167 ± 3 mV and 1073 ± 13 mV, respectively. By contrast, the output voltage of the cantilever integrated with the half-bridge configuration was 352 ± 0.002 mV at a 500 μm displacement (Fig. 5e), indicating a considerably lower output voltage than that of the full-bridge configuration. The output voltage, according to the displacement change, showed a high linearity (R^2 > 0.99), compared with our previously published nano-crack-based strain sensor. The full-bridge strain sensor-integrated cantilever exhibited ~3 times higher sensitivity than the half-bridge sensor-integrated cantilevers, as shown in Fig. S4 (a) and (b).† The proposed device showed excellent sensitivity compared with that of other published strain sensor integrated cantilever-based biosensing platforms (Table S2†). Although the crack-based sensor has high sensitivity due to the structural characteristics of the surface metal layer, the amount of change in resistance increases exponentially. Hence it is necessary to build a database to compare resistance changes according to the contractile force of myocardial cells. The Wheatstone bridge integrated multi-layered polymer cantilever is not highly sensitive as compared with the nano-crack-based sensor (Fig. S5†). However, the Wheatstone bridge strain sensor integrated multi-layered polymer cantilever exhibits excellent linearity to all the applied strain region. Owing to its outstanding linearity, the proposed device has great potential for practical use in biomedical fields. The structural stability of the multi-layered PI/PDMS cantilever was periodically monitored over 21 days (Fig. S6†). The bar plot shows no significant difference in the average thickness of each layer such as the bottom PI, sandwiched PDMS, top PI and encapsulation PI layer before and after immersion in a culture medium for 3 weeks, indicating the high structural reliability of the proposed device (Fig. S7†). The structural integrity of the Cr/Au patterned on the PI substrate was evaluated under different mechanical stresses such as bending, rolling and twisting (Fig. S8†). The LED connected to the Cr/Au was continuously glowing in all conditions, indicating the high structural integrity and robustness of the Cr/Au pattern on the PI substrate (Fig. S8c†).

3.2. Real-time contraction force measurement of the cultured cardiomyocytes

To prove the reliability and repeatability of the multi-layered polymer cantilever as a biomedical sensor, cardiomyocytes were cultured on the cantilever surface, and their contractile properties were investigated in detail as a function of time. Cardiomyocytes extracted from Sprague-Dawley rats were seeded at a density of 1000 cells mm^{-2} on the entire surface of the multi-layered polymer cantilever pre-coated with fibronectin. The cell culture medium was changed once every 72 h

during the culture period, and the maturation of cardiomyocytes was monitored through an optical microscope at specific time intervals (Fig. S9†). Fig. 5 presents the output voltage of the multi-layered polymer cantilever as a function of culture time. Fig. 5a shows the real-time trend in the strain sensor output voltage measured on day 14 after the cell seeding. We demonstrated the biocompatibility and practical applicability of the prepared multi-layered polymer cantilever by the maturation and real-time detection of the contractile behavior of the cultured cardiomyocytes. The cardiomyocytes were synchronized from the 3rd day after cell culture, and the measurement was performed for 12 days. The beat rate and contraction force of the cardiomyocytes obtained through the integrated strain were measured as a function of the culture period from day 4 to day 16 (Fig. 5b and c). The sensor output indicating the displacement change increased with the increase in the incubation time, and it reached the maximum value on day 14. The output voltages on days 5 and 14 were approximately 5.79 ± 1.07 mV and 45.66 ± 2.71 mV, respectively. Subsequently, the cantilever displacement began to decrease, and the beat rate became stable (Fig. 5b). The beating rate of the cardiomyocytes on day 4 was 1.32 ± 0.05 Hz, which gradually decreased and reached the lowest value on day 14 (0.49 ± 0.02 Hz) (Fig. 5c). The decrease in contractile behavior of the cardiomyocytes can be attributed to the aging of the cardiomyocytes on the cantilever. Another reason may be the weakening of the adhesion on the nanopatterned PDMS surface with an increase in the cardiomyocyte contraction force. The contractile force and beat rate according to the culture period are inversely proportional. The maximum displacement and its date may vary slightly depending on the characteristics and conditions of the cells growing on the polymer cantilevers.

3.3. Force–frequency relationship (FFR) of the cultured cardiomyocytes

It is important to analyze the FFR of cardiomyocytes upon application of external electrical stimulation, as the negative gradient of this relationship can indicate a lack of maturity of the cells.[14] For the electrical stimulation, we used a well-plate equipped with a pair of carbon rods connected to a function generator. The contractile force of the cardiomyocytes was characterized under various conditions of electrical stimulations (square wave pulse, 2 ms, 3 V cm^{-1}) ranging from 0.5 to 3.5 Hz at a ramping rate of 0.5 Hz, as shown in Fig. 6. The output voltage of the cantilever sensor by contraction of the cardiomyocytes was measured after stabilization at each frequency for 1 min. For electrical stimulation frequencies of 0.5, 1, 1.5, 2, 2.5, 3, and 3.5 Hz, the beat rates were exactly synchronized to 30, 60, 90, 120, 150, 180, and 210 beat min^{-1}, respectively. The cultured cardiomyocytes exhibited a negative FFR upon the application of electrical stimulation. Fig. S10† shows the real-time traces of the sensor output voltage at different applied electrical stimulations ranging from 0.5 Hz to 3 Hz. The bar graphs in Fig. 6c and d show the output voltage and relative forces generated from the cardiomyocytes under different electrical stimulations. The output voltage and relative contractile force of the cardiomyocytes decreased with increasing electrical stimulation. The relative force reduced by ~50% from the initial state when the electrical stimulation frequency was close to 2.5 Hz. In addition, when the electrical stimulation frequency was higher than 2 Hz, the cells neither completely relaxed nor completely contracted. Therefore, it was difficult to accurately analyze the displacement of the cantilever caused by the contraction and relaxation of the cardiomyocytes when the electrical stimulation frequency was higher than 2 Hz. This result indicates that if the beating frequency of cardiomyocytes is very high, it is difficult to accurately measure the contraction and relaxation forces with elastic structures such as polymer cantilevers. This problem should be considered when designing cantilevers in the future.

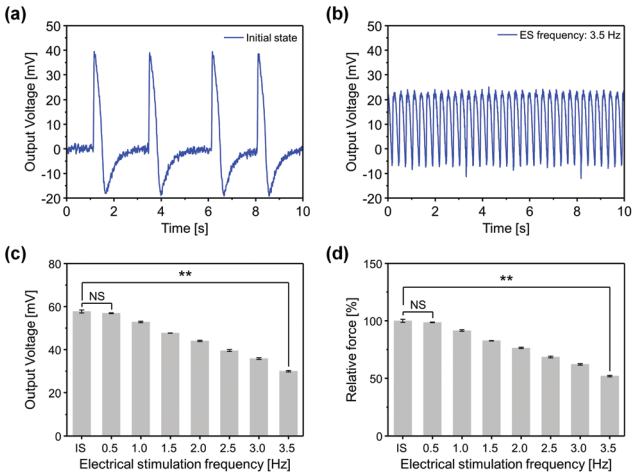

Fig. 6 Effect of external electrical stimulation (ES) on the cultured cardiomyocytes. (a) Natural beating rate of the cultured cardiomyocytes. (b) Force-beating frequency relationship in cultured cardiomyocytes under 3.5 Hz electrical stimulation. (c and d) Corresponding output voltage generated by the strain sensor and relative contraction force generated by cardiomyocytes at different applied electrical stimulation frequencies. Error bars are mean ± s.d. (n = 5 biologically independent samples); ** p < 0.01 measures by one-way ANOVA followed by Tukey's honest significant difference test. IS and NS represent initial state and non-significant.

There is a strong need to enhance the performance of mechanical contraction-based assays to improve our understanding of the risk of cardiac toxicity.

Human induced pluripotent stem cell-derived cardiomyocytes (hiPSC-CMs) are being rapidly developed for overcoming the drawbacks of animal use in drug discovery and cardiotoxicity screening. The use of hiPSC-CMs for the investigation of mechanical property changes will help characterize the expression and activity of molecules in cellular pathways known to regulate the function of cardiomyocytes. There are three important ions that affect contraction and periodic beats in animal cardiomyocytes and hiPSC-CMs. Among them, Ca^{2+} is the dominant ion affecting the contraction force of cardiomyocytes. Verapamil, a calcium channel blocker, was employed to study the relationship between drug concentration and cardiomyocyte force change, as shown in Fig. 7

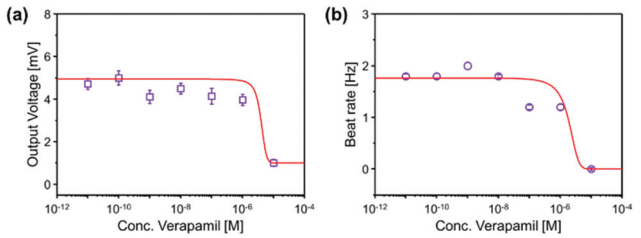

Fig. 7 Effect of verapamil on the contractility of cultured cardiomyocytes. (a and b) Drug–dose response curves indicating the inotropic and chronotropic effect of cardiomyocytes treated with different verapamil concentrations. Error bars represent the mean ± s.d. (n = 5).

and Fig. S11.† The output voltage of the polymer cantilever caused by the repetition of cardiomyocyte contraction and relaxation gradually decreased as the concentration of verapamil increased. The output voltage measured by the integrated sensor was 5.14 ± 0.31, 4.73 ± 0.25, 3.96 ± 0.26, and 0.99 ± 0.16 mV at the initial state and at 0.01 nM, 1 μM, and 10 μM verapamil, respectively; the beat rates for the same drug concentrations were 1.9 ± 0.054, 1.8 ± 0.044, 1.2 ± 0.054 Hz, and $1.2 \times 10^{-4} \pm 10^{-5}$ Hz, respectively. The beat rate of the cardiomyocytes at 10 μM decreased by ~99% compared with that for their initial state. The movement of Ca^{2+} inside and outside the cardiomyocytes was believed to have worsened with the increase in verapamil concentration. An IC_{50} (inhibitor concentration) is the statistical estimation of the drug that is required to reduce 50% of specific biological or biochemical function of the drug-induced cultured cardiomyocytes. The drug-treated hiPSC-CMs showed a negative inotropic and chronotropic effect with an IC_{50} value of 3.95×10^{-6} M and 1.93×10^{-6} M (Fig. 7 and Fig. S11†). When the hiPSC-CMs were treated with verapamil above the IC_{50} value, the contractile force and beat rate decreased because of a decrease in Vmax, the amplitude, and the conduction velocity.[15,16]

4. Conclusion

In this study, a multi-layered polymer cantilever integrated with a strain sensor was prepared and evaluated for biomedical applications. The polymer cantilever is composed of two PI (bottom and top) layers and nanopatterned PDMS layers. Each layer of the polymer is chemically bonded with the help of an interlayer (Cr/SiO_2) using oxygen plasma treatment. The strain sensor is fully encapsulated for use in liquids, and it has a full-bridge configuration that provides maximum force sensitivity. The ΔR for the strain sensor is ~91 ± 2.15 and ~272 ± 1.69 mΩ on the bottom and top PI layer, respectively. The sensitivity of the full-bridge configuration is ~2.26 mV μm^{-1}, which is ~3 times higher than that of a half-bridge configuration. The proposed cantilever sensor exhibited excellent linearity, stability, sensitivity, and reproducibility without being affected by the cell culture environment. The integrated strain sensor with the full-bridge configuration greatly simplifies data collection and analysis, and it is expected to be used as a drug toxicity screening platform with its long-term stable cell culture capability.

Author contributions

Dong-Su Kim: conceptualization; investigation; formal analysis; data curation; visualization; writing – original draft; Yun-Jin Jeong: contributed to writing the manuscript; data curation. Jongsung Park: investigation; methodology; software. Arunkumar Shanmugasundaram: investigation, writing – original draft; Dong-Weon Lee: supervised the project.; funding acquisition; supervision; conceptualization; methodology; software; validation; formal analysis; data curation; visualization; writing – original draft.

Conflicts of interest

There are no conflicts to declare.

Acknowledgements

This study was supported by a National Research Foundation of Korea (NRF) grant funded by the Korean government (MSIT) (No. 2020R1A5A8018367) and by the Basic Science Research Program by the National Research Foundation of Korea (NRF) funded by the Ministry of Education (No. 2019R1A6A3A13095692).

References

1 C. Ziegler, *Anal. Bioanal. Chem.*, 2004, **379**, 946–959.
2 J. Y. Kim, Y.-S. Choi, B.-K. Lee and D.-W. Lee, *Biosens. Bioelectron.*, 2016, **80**, 456–462.
3 Y. Dai, N.-E. Oyunbaatar, B.-K. Lee, E.-S. Kim and D.-W. Lee, *Sens. Actuators, B*, 2018, **255**, 3391–3399.
4 N.-E. Oyunbaatar, A. Shanmugasundaram, Y.-J. Jeong, B.-K. Lee, E.-S. Kim and D.-W. Lee, *Colloids Surf., B*, 2020, **186**, 110682.
5 P. P. Kanade, N.-E. Oyunbaatar and D.-W. Lee, *Micromachines*, 2020, **11**, 450.
6 D.-S. Kim, Y.-J. Jeong, A. Shanmugasundaram, N.-E. Oyunbaatar, J. Park, E.-S. Kim, B.-K. Lee and D.-W. Lee, *Biosens. Bioelectron.*, 2021, 113380.
7 A. W. Feinberg, A. Feigel, S. S. Shevkoplyas, S. Sheehy, G. M. Whitesides and K. K. Parker, *Science*, 2007, **317**, 1366–1370.
8 D.-S. Kim, Y.-J. Jeong, B.-K. Lee, A. Shanmugasundaram and D.-W. Lee, *Sens. Actuators, B*, 2017, **240**, 566–572.
9 D.-S. Kim, Y. W. Choi, A. Shanmugasundaram, Y.-J. Jeong, J. Park, N.-E. Oyunbaatar, E.-S. Kim, M. Choi and D.-W. Lee, *Nat. Commun.*, 2020, **11**, 1–13.
10 J. U. Lind, M. Yadid, I. Perkins, B. B. O'Connor, F. Eweje, C. O. Chantre, M. A. Hemphill, H. Yuan, P. H. Campbell and J. J. Vlassak, *Lab Chip*, 2017, **17**, 3692–3703.

11 J. U. Lind, T. A. Busbee, A. D. Valentine, F. S. Pasqualini, H. Yuan, M. Yadid, S.-J. Park, A. Kotikian, A. P. Nesmith and P. H. Campbell, *Nat. Mater.*, 2017, **16**, 303–308.
12 K. Matsudaira, T.-V. Nguyen, K. H. Shoji, T. Tsukagoshi, T. Takahata and I. Shimoyama, *J. Micromech. Microeng.*, 2017, **27**, 105005.
13 A. Johansson, M. Calleja, P. Rasmussen and A. Boisen, *Sens. Actuators, A*, 2005, **123**, 111–115.
14 M. Endoh, *Eur. J. Pharmacol.*, 2004, **500**, 73–86.
15 M. R. Rosen, J. P. Ilvento, H. Gelband and C. Merker, *J. Pharmacol. Exp. Ther.*, 1974, **189**, 414–422.
16 N. Szentandrássy, D. Nagy, B. Hegyi, J. Magyar, T. Bányász and P. P. Nanasi, *Curr. Pharm. Des.*, 2015, **21**, 977–1010.